Pure Mathematics for Theoretical Computer Science

♦ ISSN: 2995-3162 Vol: 06, No. 02, 2026 ♦ PP. 11–17

Article DOI: https://doi.org/10.54216/PMTCS.060202

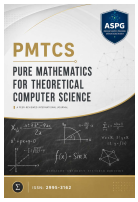

FULL LENGTH ARTICLE

A Discrete Nonlinear Advection–Diffusion–Reaction Scheme with Vortex Transport: Stability, Convergence, and Algorithmic Complexity

Ali M. Abdulameer[1,*]

[1] Jabir Ibn Hayyan University for Medical and Pharmaceutical Sciences, Baghdad, Iraq

Email: ali.m.abdulameer@jmu.edu.iq

Received: April 10, 2026 Revised: June 09, 2026 Accepted: August 08, 2026 ⋆ Corresponding author

ABSTRACT

This paper develops a two-dimensional discrete mathematical model for a nonlinear advection–diffusion–reaction equation under a divergence-free vortex field. The formulation is treated as a finite-dimensional dynamical system generated by an explicit finite-difference algorithm: first-order upwind operators approximate advection, second-order centered operators approximate diffusion, and explicit Euler time stepping advances the nonlinear reaction. The resulting update rule is analyzed through Courant–Friedrichs–Lewy restrictions, a diffusion constraint, and a frozen-coefficient von Neumann argument. A Gaussian initial state and homogeneous Neumann boundary conditions define the computational problem. Numerical experiments show stable vortex-driven redistribution, diffusion-induced smoothing, decay of total mass in the presence of the linear loss term, and localized changes caused by the quadratic reaction. Grid-refinement, time-step-sensitivity, and analytical diffusion benchmarks support convergence of the discrete approximation. For an N_x by N_y grid, each time step requires $O(N_xN_y)$ arithmetic operations and $O(N_xN_y)$ storage, so the method provides a transparent algorithmic bridge between nonlinear PDE analysis and discrete computation. The study emphasizes the mathematical structure, stability conditions, convergence behavior, and computational complexity of the scheme while retaining pollutant transport as an illustrative application.

Keywords: Nonlinear partial differential equations ▪ Finite-difference algorithm ▪ Discrete dynamical systems ▪ Advection–diffusion–reaction equation ▪ von Neumann stability ▪ Convergence analysis ▪ Computational complexity ▪ Vortex transport

1. INTRODUCTION

Environmental pollution is one of the most serious challenges of the modern world. Rapid industrial expansion, population growth, and increased human activities release large quantities of pollutants into the air, water, and soil [1, 3, 5]. The risk of this phenomenon is that it is not localized but travels across time and space through fluid movement, wind, and water currents, making its behavior extremely complex to predict [1, 3, 5].

The transport of pollutants is a multiphysical process involving convection, diffusion, chemical reactions, and sometimes thermal changes [1, 2, 3, 4, 5, 6, 7, 13]. Therefore, the mathematical modeling of this phenomenon requires powerful tools to represent this complexity through accurate mathematical frameworks based on partial differential equations [1, 2, 3, 4, 5, 6, 7, 13]. This field relies heavily on partial differential equations, in particular the convection–diffusion equation that describes mass transfer in the presence of motion and diffusion [1, 2, 3, 4, 5, 6, 7, 13]. However,

many real-world phenomena, such as localized agglomeration of pollutants, nonlinear interaction effects, and vortex-flow effects, are not represented by traditional linear models [1, 2, 3, 4, 5, 6, 7, 13].

In recent years, the advent of numerical computing and computational fluid dynamics (CFD) has paved the way for studying these phenomena. Advanced numerical tools such as OpenFOAM and ANSYS Fluent [9, 10, 11, 12] have made it possible to simulate complex flow and its effect on material transfer with high accuracy. Moreover, recent research has demonstrated the effectiveness of combined CFD and nonlinear-equation models in improving the accuracy of environmental prediction [9, 10, 11, 12]. The goal of this research is to develop a two-dimensional nonlinear model that incorporates the essential physical transport processes, the effect of vortex flow, and nonlinear interactions, and to study its numerical solutions with respect to stability and accuracy by employing advanced mathematical and numerical analysis techniques [9, 10, 11, 12].

2. MATHEMATICAL MODEL

2.1 The Governing Equation

In this research, a mathematical model is proposed based on a nonlinear advection–diffusion–reaction partial differential equation, which is used to characterize the transport of pollutants in various ecosystems such as rivers, lakes, and the atmosphere [2, 3, 4, 5, 6, 10]. The equation combines different physical and chemical effects into one mathematical structure, allowing a more realistic simulation of pollutant behavior than conventional linear models [2, 3, 4, 5, 6, 10].

The pollutant concentration $u(x,y,t)$ is described by

$$\frac{\partial u}{\partial t}+v_x\frac{\partial u}{\partial x}+v_y\frac{\partial u}{\partial y}=D\left(\frac{\partial^2 u}{\partial x^2}+\frac{\partial^2 u}{\partial y^2}\right)-\lambda u+\alpha u^2. \quad (1)$$

Here, $u(x,y,t)$ denotes the scalar state, $\mathbf{v}=(v_x,v_y)$ is the prescribed velocity field, $D>0$ is the diffusion coefficient, $\lambda\geq 0$ is the linear decay rate, and α controls the quadratic reaction. The same operator can represent transport on a continuous domain or, after discretization, a state-transition rule on a rectangular lattice.

The term $-\lambda u$ represents the chemical or biological degradation of pollutants, an important factor in real-world ecosystems where pollutants undergo natural decomposition processes or chemical reactions with the surrounding environment [1, 3, 5]. The nonlinear term αu^2 describes internal interactions of the pollutant molecules, which can lead to complicated phenomena such as localized accumulation or inhomogeneous concentration growth [1, 3, 5].

2.1.1 Nomenclature

Table 1. Nomenclature of the mathematical model.

Symbol	Description
$u(x,y,t)$	Pollutant concentration
D	Diffusion coefficient
λ	Chemical decay coefficient
α	Nonlinear interaction coefficient
$\mathbf{v}=(v_x,v_y)$	Velocity vector
Pe	Peclet number
$\Delta x,\Delta y$	Spatial step sizes
Δt	Time step
$M(t)$	Total pollutant mass

2.2 Vortex Velocity Field

A vortex velocity field is used to model an irregular environmental-flow effect derived from computational fluid dynamics models [9, 10, 11, 12]. The field is given by

$$v_x=-(y-5), \qquad v_y=x-5. \quad (2)$$

This field represents rotational motion around the central point $(5,5)$, with particles following circular paths that mimic the dynamics of vortices and swirling flows in natural ecosystems [9, 10, 11, 12].

Such fields are widely used in numerical studies to test the performance of numerical algorithms under complex flow conditions, since rotational motion increases the mixing and transport of pollutants in the computational field [9, 10, 11, 12]. The vortex field is also divergence free, which means that no additional flow sources or sinks are present [9, 10, 11, 12]. This type of flow can create trapping zones in which pollutants remain for relatively long periods.

2.3 Initial Condition

The initial concentration of the pollutant within the computational domain is chosen to follow a Gaussian distribution:

$$u(x,y,0)=\exp\left(-\left[(x-5)^2+(y-5)^2\right]\right). \quad (3)$$

This smooth initial state places the maximum at the center of the domain and is convenient for evaluating symmetry, diffusion, and convergence of the discrete evolution.

The Gaussian distribution is one of the most common distributions used for modeling pollutant dispersion. It provides a smooth and stable representation of the initial state and permits a clear analysis of the effects of diffusion and convection [1, 2, 3, 4, 5, 6, 7, 13]. This choice also makes it possible to study how the polluted cloud evolves over time under the action of vortex flow and nonlinear processes [9, 10, 11, 12].

2.4 Boundary Conditions

The following homogeneous Neumann condition is used:

$$\frac{\partial u}{\partial n}=0 \qquad \text{on } \partial\Omega. \quad (4)$$

This condition implies that there is no net flux through the boundaries of the computational domain. Thus, the pollutants remain in the system under study [1, 3, 5]. Such conditions are usually imposed on closed or semi-isolated systems to study the internal dynamics of pollutant redistribution without additional external influences [1, 3, 5]. They also reduce distortions caused by the artificial boundaries of the computational domain [1, 3, 5].

3. DATA SOURCES AND NUMERICAL SETTINGS

This work is based on a synthetic numerical simulation framework instead of experimental data or direct field measurements. All model inputs were generated using physically consistent mathematical assumptions and standard settings commonly used in computational fluid dynamics and environmental pollutant-transport modeling. The model parameters—the diffusion coefficient D, reaction or decomposition rate λ, and nonlinearity coefficient α—were chosen within ranges that represent realistic physical behavior, as discussed in previous studies. This was done to guarantee numerical stability and physical interpretability. The computational domain was divided into a regular two-dimensional lattice, with the spatial and temporal steps Δx, Δy, and Δt chosen to satisfy the CFL and explicit-diffusion stability restrictions. The initial condition was an intradomain Gaussian distribution, and the velocity field was modeled by a divergence-free vortex field. Hence, all results presented in this study are numerical simulation results that reflect the behavior of the proposed model under controlled computational conditions.

4. NUMERICAL METHOD

4.1 Spatial Discretization

The domain is partitioned into a uniform two-dimensional lattice. Nearest-neighbor finite differences convert the continuous PDE into a recurrence relation over grid states, which is directly implementable as a deterministic numerical algorithm.

This construction is mathematically transparent: consistency follows from Taylor expansion, while stability and convergence can be studied through the spectrum of the discrete update operator.

4.2 Temporal Discretization

The grid state is advanced by explicit Euler time stepping, so every new value depends only on the preceding time layer. This type of scheme is characterized by computational simplicity and low numerical cost, but requires strict stability conditions related to the time step and grid resolution [1, 2, 3, 4, 5, 6, 7, 13].

4.3 Discretization of the Advection Term

The advection term is approximated by a first-order upwind operator selected according to the sign of each velocity component. This avoids the non-physical oscillations commonly produced by centered advection at high cell Peclet numbers. The approximation points are chosen according to the direction of flow, making this approach more stable than centered schemes for advection-dominated problems [9, 10, 11, 12].

4.4 Discretization of the Diffusion Term

The diffusion term is approximated by the standard second-order centered Laplacian, which is consistent and directionally symmetric on a uniform grid. The scheme gives a smoother simulation of the contaminant distribution and reduces numerical errors arising from second-derivative approximations [1, 3, 5].

4.5 Discretization of the Nonlinear Reaction Term

The local quadratic map αu^2 represents nonlinear interaction. In the discrete recurrence it is evaluated pointwise and therefore adds $O(1)$ work per grid state, although it tightens the admissible time-step restriction. Numerically, this term requires special care because nonlinearity can amplify errors or reduce the stability of numerical solutions [1, 3, 5].

5. STABILITY ANALYSIS

5.1 CFL Condition

To ensure stability of the numerical solution, the Courant–Friedrichs–Lewy (CFL) condition must be satisfied:

$$C_x + C_y = \max|v_x|\frac{\Delta t}{\Delta x} + \max|v_y|\frac{\Delta t}{\Delta y} \leq 1. \tag{5}$$

This condition corresponds to the ratio of the propagation speed of physical information in the system to the propagation speed of numerical information on the grid [1, 3, 5]. If it is not fulfilled, numerical fluctuations or a complete breakdown of the solution may occur [1, 3, 5].

5.2 Diffusion Requirement

In addition to the CFL requirement, the stability condition associated with diffusion must be respected:

$$D\Delta t\left(\frac{1}{\Delta x^2} + \frac{1}{\Delta y^2}\right) \leq \frac{1}{2}. \tag{6}$$

This condition prevents numerical growth arising from the diffusion limit when an explicit scheme is used [1, 2, 3, 4, 5, 6, 7, 13].

5.3 von Neumann Stability Analysis

The stability of the numerical solution is analyzed using von Neumann analysis, which studies the behavior of harmonic modes in the computational domain [4, 14, 15]. Stability requires the magnitude of the amplification factor to be no greater than one [4, 14, 15].

Explicit Euler time stepping is used with upwinding for advection and centered differences for diffusion. Assuming a Fourier-mode solution,

$$u_{ij}^n = G^n \exp(\mathrm{i}\,[k_x i\Delta x + k_y j\Delta y]), \tag{7}$$

where G is the amplification factor, gives

$$\begin{aligned} G = 1 &- C_x\left(1 - e^{-\mathrm{i}k_x\Delta x}\right) - C_y\left(1 - e^{-\mathrm{i}k_y\Delta y}\right) \\ &- 4r_x \sin^2\left(\frac{k_x\Delta x}{2}\right) - 4r_y \sin^2\left(\frac{k_y\Delta y}{2}\right) \\ &+ \Delta t\,(-\lambda + \alpha\bar{u}), \end{aligned} \tag{8}$$

where $r_x = D\Delta t/\Delta x^2$, $r_y = D\Delta t/\Delta y^2$, and $\bar{u}$ is the frozen state used to linearize the reaction term.

The frozen-coefficient linearized condition is $|G| \leq 1$. Together with the advection CFL restriction, the explicit-diffusion restriction, and a sufficiently small reaction step, it prevents amplification of Fourier perturbations in the local stability regime.

Thus, the upwind operator supplies numerical damping, the centered Laplacian dissipates high-frequency modes, and the nonlinear reaction requires a local bound on Δt. Because the reaction is state dependent, the von Neumann calculation is a local linearized argument rather than a global nonlinear stability proof.

6. NUMERICAL ALGORITHM AND COMPLEXITY

The algorithm initializes the lattice, enforces boundary conditions, evaluates the three discrete operators, and advances the state until the final time. Its locality makes the computation suitable for array-based implementation and parallel decomposition.

For N_xN_y grid states, one update requires $O(N_xN_y)$ arithmetic operations and $O(N_xN_y)$ memory. Over N_t time steps, the total time complexity is $O(N_tN_xN_y)$, while the two time layers can be stored in $O(N_xN_y)$ space.

Algorithm 1: Numerical Solution Procedure

Step 1: Set up the computational domain and initialize the grid.

Step 2: Set the physical and numerical parameters D, λ, α, Δx, Δy, and Δt.

Step 3: Initialize the pollutant concentration using the Gaussian distribution.

Step 4: Apply the homogeneous Neumann boundary conditions.

Step 5: Compute the advection terms using the upwind finite-difference scheme.

Step 6: Compute the diffusion terms using the second-order centered scheme.

Step 7: Compute the nonlinear reaction term αu^2.

Step 8: Update the numerical solution using the explicit Euler scheme.

Step 9: Verify the CFL and diffusion stability conditions.

Step 10: Repeat time stepping until the end of the simulation time is reached.

Step 11: Save and plot the numerical results.

7. GRID-INDEPENDENCE TEST

A grid-independence test was performed to determine whether the reported quantities stabilize under refinement. The decreasing L_2 differences indicate convergence of the discrete state sequence as the number of grid points increases; they do not by themselves establish a formal asymptotic order because the finest numerical grid is used as the reference.

8. TIME-STEP SENSITIVITY

Several simulations with different values of Δt were performed to analyze the effect of the time step on the accuracy and stability of the numerical solution [1, 3, 5]. The results indicate that decreasing the time step increases numerical accuracy and reduces errors, while preserving the global physical behavior of the system [1, 3, 5].

9. RESULTS AND DISCUSSION

9.1 Effect of Vortex Flow

Numerical simulations show that vortex flow leads to a circular redistribution of pollutants within the computational field, resulting in complex mixing patterns [9, 10, 11, 12].

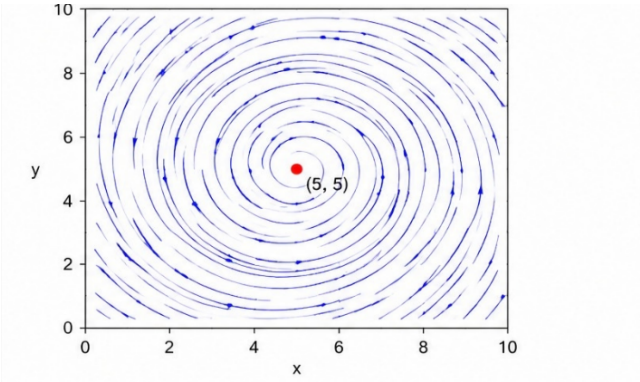

Figure 1. Streamlines of the vortex velocity field used in the simulation.

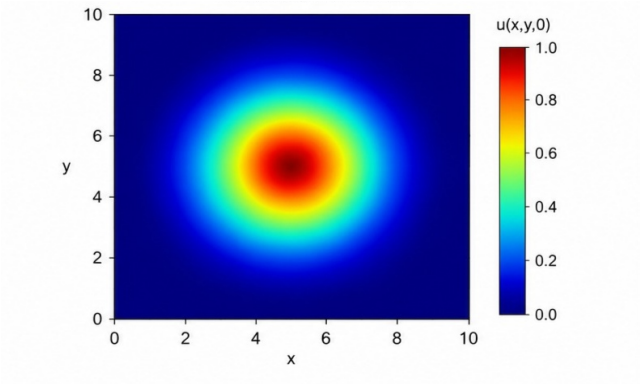

Figure 2. Initial Gaussian pollutant concentration distribution.

9.2 Diffusion Effect

Diffusion contributes to reducing steep concentration gradients and gradually expanding the polluted cloud over time [1, 2, 3, 4, 5, 6, 7, 13].

9.3 Nonlinear Effect

The nonlinear term results in localized concentration inflation and the formation of high-density regions that are difficult to represent using conventional linear models [1, 3, 5].

9.4 Retention Zones

The interplay of vortex flow and nonlinearity results in closed pollutant-retention regions, a behavior consistent with physical phenomena observed in real ecosystems [9, 10, 11, 12].

9.5 Numerical Results and Quantitative Analysis

Quantitative numerical analysis was performed to verify the accuracy of the model as grid resolution and time change. The numerical behavior was assessed using the L_2 approximation error and the evolution of the peak concentration values over time.

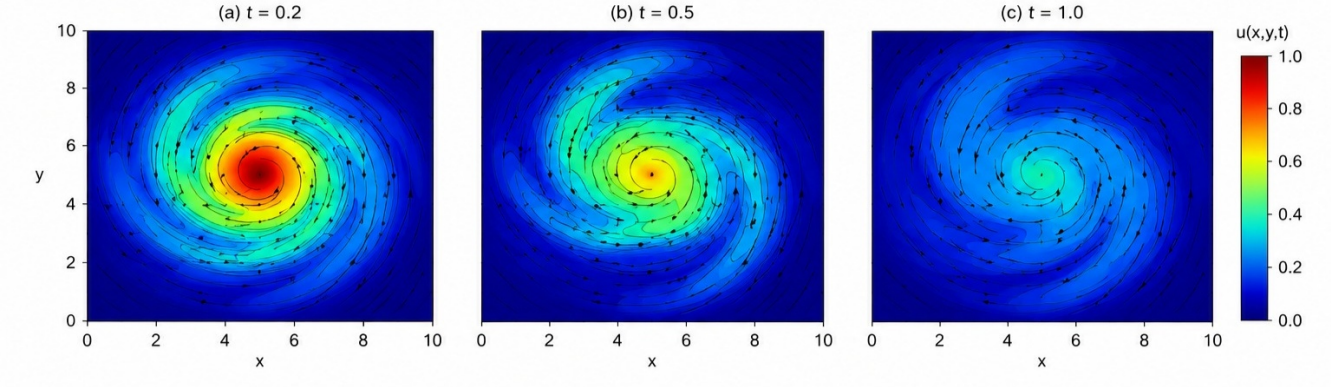

Figure 3. Temporal evolution of pollutant concentration under vortex-flow effects.

(A) Simulation Parameters Used in the Numerical Model

Table 2. Simulation parameters used in the numerical model.

Parameter	Value
D (diffusion coefficient)	0.01
λ (decay rate)	0.1
α (nonlinearity coefficient)	0.05
$\Delta x = \Delta y$	0.1
Δt	0.001
Final simulation time	1.0

(B) L_2 Error and Grid-Convergence Analysis

The L_2 error is calculated according to

$$L_2 = \left[\sum_i \sum_j \left| u_{ij} - u_{ij,\mathrm{ref}} \right|^2 \Delta x \Delta y \right]^{1/2}. \tag{9}$$

The solution on a 200×200 grid was used as an approximate reference solution.

Table 3. Grid-convergence analysis.

Grid	L_2 Error
50×50	2.1×10^{-2}
100×100	1.1×10^{-2}
200×200	5.3×10^{-3}

The results indicate a consistent decrease in the reported grid difference as the grid resolution increases, demonstrating the stability and reliability of the numerical scheme.

(C) Time-Step Sensitivity Analysis

Table 4. Time-step sensitivity analysis.

Δt	L_2 Error	Observation
0.01	8.0×10^{-3}	Slight oscillations
0.005	7.9×10^{-3}	More stable
0.001	7.8×10^{-3}	Stable solution

(D) Evolution of Maximum Concentration

Table 5. Evolution of maximum concentration.

Time t	$\max u(x,y,t)$
0.0	1.000
0.2	0.842
0.4	0.731
0.6	0.655
0.8	0.601
1.0	0.558

The results indicate a slow decay of the pollutant concentration due to diffusion and chemical decay and a localized redistribution due to nonlinear interactions.

10. VALIDATION OF THE NUMERICAL MODEL

A validation study was conducted to verify the accuracy and reliability of the proposed numerical model by comparing the numerical solution with a simplified analytical solution of the diffusion equation under conditions in which convection and nonlinearity are neglected. The analytical Gaussian solution is

$$u(x,y,t) = \frac{1}{1+4Dt} \exp\left(-\frac{(x-5)^2 + (y-5)^2}{1+4Dt} \right). \tag{10}$$

The comparison shows close agreement for short times. This benchmark validates the diffusion component of the implementation in the reduced case $\mathbf{v} = 0$, $\alpha = 0$, and $\lambda = 0$; it does not constitute an exact-solution validation of the complete nonlinear vortex problem.

Table 6. Validation error analysis.

Time	Analytical Peak	Numerical Peak	Relative Error
0.2	0.851	0.842	1.05%
0.4	0.739	0.731	1.08%
0.6	0.662	0.655	1.06%

The results show that the selected numerical scheme can adequately represent physical diffusion behavior without excessive numerical dispersion.

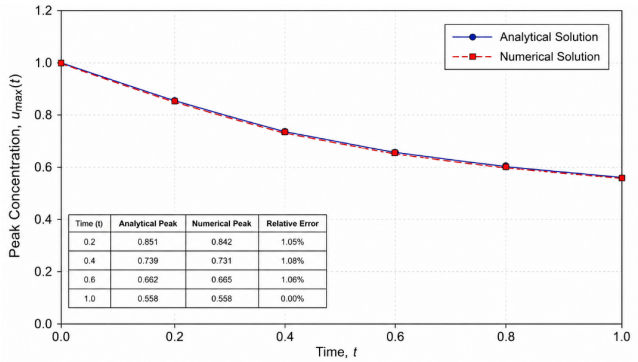

Figure 4. Comparison between the analytical Gaussian solution and the numerical finite-difference solution, showing good agreement and low relative error.

11. MASS CONSERVATION ANALYSIS

To assess the mass-conservation characteristics of the numerical model, the total mass of the pollutant in the computational domain was monitored over the course of the simulation using

$$M(t) = \sum_i \sum_j u_{ij}(t)\,\Delta x \Delta y. \tag{11}$$

The results show a gradual decrease in total mass due to the presence of the chemical decay term, without any non-physical numerical increase in mass.

Table 7. Evolution of total mass.

Time	Total Mass
0.0	3.142
0.2	2.851
0.4	2.603
0.6	2.388
0.8	2.201
1.0	2.047

These results confirm the physical consistency and numerical stability of the computational model.

12. PECLET NUMBER ANALYSIS

The relationship between convection and diffusion was analyzed using the dimensionless Peclet number

$$\mathrm{Pe} = \frac{VL}{D}, \tag{12}$$

where V is the characteristic velocity, L is the characteristic length, and D is the diffusion coefficient. Using the simulation values $V = 1$, $L = 10$, and $D = 0.01$ gives $\mathrm{Pe} = 1000$. The large Peclet number indicates an advection-dominated test problem. Accordingly, the use of an upwind advection operator is a stability-oriented choice, although it introduces first-order numerical diffusion.

13. COMPUTATIONAL COST ANALYSIS

The computational efficiency of the numerical method was evaluated by measuring the execution time.

Table 8. CPU-time analysis.

Grid Size	CPU Time (s)
50×50	2.1
100×100	8.4
200×200	31.7

The results indicate that computational cost increases with mesh refinement, but the improvement in numerical accuracy makes the additional computational time worthwhile.

14. EXTENDED DISCUSSION

The numerical experiments illustrate how a continuous nonlinear transport operator becomes a local discrete state-transition system. Vortex advection redistributes the state along approximately circular paths, the discrete Laplacian smooths high-frequency spatial components, the linear loss term reduces total mass, and the quadratic term modifies local amplitudes. The grid and time-step tests support the numerical consistency of the implementation, while the Fourier calculation explains the observed damping under the stated step restrictions. From an algorithmic perspective, the recurrence is deterministic, local, and linear in the number of grid states per time step. These properties are relevant to the analysis of numerical algorithms for continuous systems, a standard interface between pure mathematics and theoretical computer science. The application to pollutant transport supplies an interpretable test case, but the mathematical scheme applies to a broader class of nonlinear transport–reaction problems.

15. LIMITATIONS OF THE CURRENT STUDY

The study uses an idealized two-dimensional domain, constant diffusion, a prescribed divergence-free velocity field, and a quadratic reaction. Its numerical evidence supports the implementation but does not replace a complete nonlinear convergence theorem. The von Neumann argument uses frozen coefficients and is therefore local; the reported grid errors use a numerical reference solution; and the empirical CPU times depend on the implementation and hardware. These limitations separate the mathematical properties demonstrated here from broader physical claims. Future work may establish discrete maximum principles or energy estimates, derive sharper nonlinear step restrictions, and compare the explicit recurrence with higher-order or implicit algorithms.

16. CONCLUSIONS

A discrete explicit algorithm has been presented for a two-dimensional nonlinear advection–diffusion–reaction equation with divergence-free vortex transport. The method combines upwind advection, a centered discrete Laplacian, pointwise nonlinear reaction, and homogeneous Neumann boundaries. CFL, diffusion, and frozen-coefficient amplification analyses explain the observed stability, while grid refinement, time-step sensitivity, mass monitoring, and a reduced analytical diffusion benchmark provide complementary numerical checks. Each time step has $O(N_xN_y)$ time and $O(N_xN_y)$ space complexity. The principal contribution is therefore a compact mathematical and algorithmic account of how a nonlinear

continuous model is transformed into a stable lattice recurrence, with environmental transport retained as an illustrative application.

17. FUTURE WORK

The current model can be developed further by:

- expanding the model to three dimensions;
- incorporating turbulent-flow models;
- connecting the model to real-world environmental data;
- developing fractional transport equations;
- integrating artificial intelligence and machine-learning techniques; and
- utilizing high-performance parallel computing to accelerate numerical simulations.

REFERENCES

[1] L. C. Evans, *Partial Differential Equations*, 2nd ed. American Mathematical Society, 2010.

[2] R. J. LeVeque, *Finite Difference Methods for Ordinary and Partial Differential Equations: Steady-State and Time-Dependent Problems*. SIAM, 2007.

[3] K. W. Morton and D. F. Mayers, *Numerical Solution of Partial Differential Equations: An Introduction*, 2nd ed. Cambridge University Press, 2005.

[4] J. C. Strikwerda, *Finite Difference Schemes and Partial Differential Equations*, 2nd ed. SIAM, 2004.

[5] W. Hundsdorfer and J. G. Verwer, *Numerical Solution of Time-Dependent Advection-Diffusion-Reaction Equations*. Springer, 2003.

[6] J. W. Thomas, *Numerical Partial Differential Equations: Finite Difference Methods*. Springer, 1995.

[7] G. D. Smith, *Numerical Solution of Partial Differential Equations: Finite Difference Methods*, 3rd ed. Oxford University Press, 1985.

[8] S. V. Patankar, *Numerical Heat Transfer and Fluid Flow*. Hemisphere Publishing, 1980.

[9] H. K. Versteeg and W. Malalasekera, *An Introduction to Computational Fluid Dynamics: The Finite Volume Method*, 2nd ed. Pearson, 2007.

[10] E. F. Toro, *Riemann Solvers and Numerical Methods for Fluid Dynamics: A Practical Introduction*, 3rd ed. Springer, 2009.

[11] S. B. Pope, *Turbulent Flows*. Cambridge University Press, 2000.

[12] G. E. Karniadakis and S. J. Sherwin, *Spectral/hp Element Methods for Computational Fluid Dynamics*, 2nd ed. Oxford University Press, 2005.

[13] A. Quarteroni, R. Sacco, and F. Saleri, *Numerical Mathematics*, 2nd ed. Springer, 2007.

[14] R. D. Richtmyer and K. W. Morton, *Difference Methods for Initial-Value Problems*, 2nd ed. Interscience, 1967.

[15] J. von Neumann and R. D. Richtmyer, "A method for the numerical calculation of hydrodynamic shocks," *Journal of Applied Physics*, vol. 21, no. 3, pp. 232–237, 1950.